Two-level atom witness of thermalization of multimode optical fibers

M. Wanic,[1] R. Khomeriki,[2] S. Stagraczyński,[1] M. I. Katsnelson,[3] Z. Toklikishvili,[2] and L. Chotorlishvili[1]

[1] *Department of Physics and Medical Engineering, Rzeszów University of Technology, 35-959 Rzeszów, Poland*

[2] *Faculty of Exact and Natural Sciences, Tbilisi State University, Chavchavadze av.3, 0128 Tbilisi, Georgia*

[3] *Radboud University, Institute for Molecules and Materials, Heyendaalseweg 135, 6525AJ Nijmegen, Netherlands*

(Dated: October 23, 2024)

In the present project, we study the dynamics of the two-level system coupled with the multimode optical system. In particular, we considered a square lattice of optical fibers. We aimed to answer whether we can infer information about the thermalization of optical modes through the thermalization of two-level atoms. After averaging over the set of modes, the dynamic of the two-level system is free of quantum revivals, and that is the signature of thermalization. We showed that the temperature of the two-level system increases with the temperature of optical modes and mean photon number. In the high-temperature limit of optical modes, the temperature of the level system tends to be infinity, and level populations are equal.

arXiv:2410.01416v1 [physics.optics] 2 Oct 2024

Since the seminal work by Mark Srednicki [1], the problem of thermalization of the isolated quantum mechanical systems is the focus of interest. Open quantum systems thermalize due to contact with the thermostat [2, 3]. However, thermalization of the isolated quantum system with many degrees of freedom is a more intriguing process [4]. Considerable attention has been paid to the thermalization process in multimode optical fiber systems in the last few years [5, 6]. In such systems, thermalization is a consequence of nonlinear photon-photon interactions. Moreover, thermalization was observed experimentally in the photonic time-synthetic mesh lattices [7]. In the present work, we are interested in the question of whether the quantum two-level system can witness the thermalization process in the multimodal optical fiber system. To answer this question, we consider Jaynes Cummings (JC) atom interacting with the set of optical modes. Since which particular mode atom couples with is inaccessible information, we consider averaging procedure over the set of modes. Typically, the JC system interacting with a coherent quantized field is characterized by quantum revivals in level populations. The quantum revival of level populations is the signature of unitary and time-reversible quantum dynamics. However, in what follows, we will prove the absence of quantum revivals after averaging the atom's dynamic over the ensemble of optical modes. The absence of revivals is the essence of thermalization of the atom. Hence, in our scenario the two-level atom interacting with the ensemble of optical modes thermalizes to a specific temperature T_a and witnesses the thermalization of optical modes.

Let us present the initial state of the quantum system as the linear superposition of eigenstates α of its Hamiltonian $\hat{H}$ corresponding to the energies E_α: $|\Psi(0)\rangle = \sum_\alpha c_\alpha |\alpha\rangle$. Then, the expectation value of the operator $\hat{\mathcal{A}}$ calculated through the evolved in time quantum state $|\Psi(t)\rangle = e^{-it\hat{H}}|\Psi(0)\rangle$, reads: $\langle\hat{\mathcal{A}}\rangle = \langle\Psi(t)|\hat{\mathcal{A}}|\Psi(t)\rangle = \sum_{\alpha,\beta} c^*_\alpha c_\beta (\hat{\mathcal{A}})_{\alpha\beta} e^{-i\omega_{\alpha\beta}t}$. The eigenstate thermalization hypothesis (ETH) argues that [8] at times $t \gg 1/\min\{\omega_{\alpha\beta}\}$, $\omega_{\alpha\beta} = (E_\alpha - E_\beta)/\hbar$ the mean value approaches to $\langle\hat{\mathcal{A}}\rangle = \sum_\alpha |c_\alpha|^2 (\hat{\mathcal{A}})_{\alpha\alpha}$ meaning that contribution of the non-diagonal terms is marginal in the large time limit $\sum_{\alpha\neq\beta} c^*_\alpha c_\beta (\hat{\mathcal{A}})_{\alpha\beta} e^{-i\omega_{\alpha\beta}t} \to 0$. It is assumed that the dimension of the system's Hilbert space is finite but large. Currently, up-to-date cold atomic gases are considered a unique platform for testing the ETH hypothesis [9–14]. In the present work, we propose an experimentally feasible system that could serve as an alternative platform when testing the fundamental principles of the ETH hypothesis. Namely, we consider a multimode optical system coupled to the JC system. We exploit the JC subsystem for quantum metrological purposes since, through the JC subsystem and experimentally accessible level dynamics, we extract information about the thermalization of the multimode optical subsystem.

Thermodynamics in the last two decades has experienced progress, and the rise of new directions, such as non-equilibrium thermodynamics of small systems and quantum thermodynamics [15–19]. In the case of quantum systems, along with fluctuations in quantum thermodynamics, quantum effects play a dominant role [20–33]. Only recently have researchers been attracted to the thermodynamic theory of highly multimode nonlinear optical systems. In this context, we admit works published during the last few years [7, 34, 35]. Without claiming to be exhaustive, we briefly recall the peculiarities of thermodynamics of highly multimode nonlinear optical systems [5–7, 34, 35]. The conserved internal energy of the optical multimode system is defined through the expectation value of the linear Hamiltonian $U = -H_L$ where $H_L = \langle\Psi|\hat{H}_L|\Psi\rangle$ and the state vector is the solution of the effective Schrödinger equation $id|\psi\rangle/dz = -\hat{H}_L|\psi\rangle$, z being a spatial coordinate. The essence of the effective Schrödinger equation is that the propagation of wave along $\hat{\mathbf{z}}$ axis mimics the evolution in time. In what follows, we consider the conceptual problem of thermaliza-

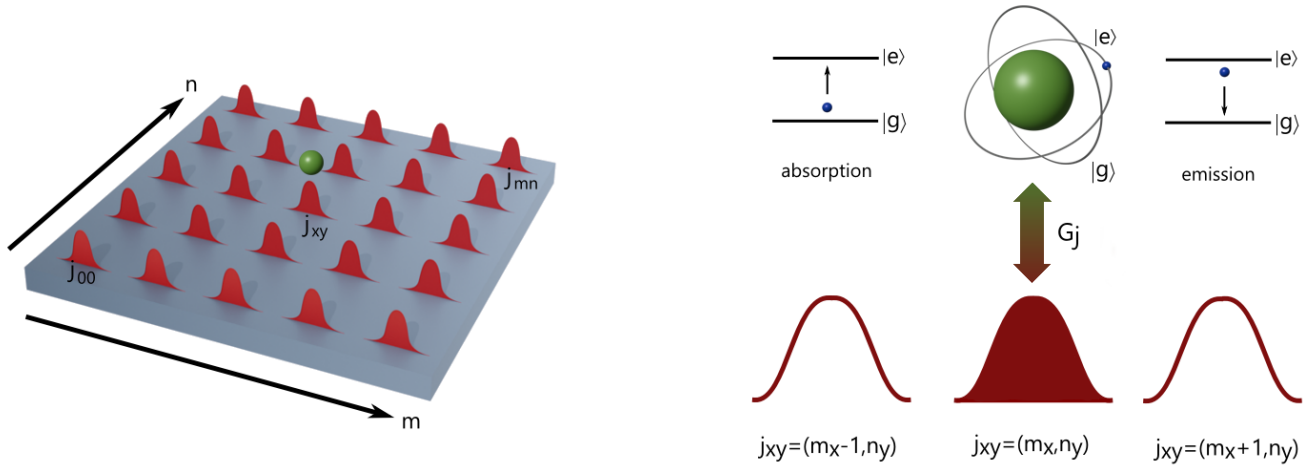

FIG. 1. Schematics of the proposed system. The multimode optical system is shown on the left side, where j_{xy} corresponds to a single mode, with n and m being integers from 1 to N, the total number of modes is equal to $N^2 = 400$. The interaction G_j between Jaynes-Cummings two-level atoms with the particular mode is shown on the right side. $|e\rangle$ and $|g\rangle$ correspond to the excited and ground state of the atom. We are unaware to which particular mode atom is coupled. Therefore, we average the dynamics of level populations of the atom over the ensemble of all modes.

tion of a two-level atom coupled with the multimode optical system. For our goal, it is sufficient to consider a $N \times N$ square lattice (see Fig.1). The eigenmodes of the multimode optical system in the context of a square lattice of optical fibers with $\hat{\mathbf{z}}$ propagation direction reads:

$$\psi_j = c_j e^{-i(\Omega t - k_0 z - \varepsilon_j z)} \tag{1}$$

where $\varepsilon_j = \delta k(\cos p + \cos q)$ (with $\delta k \ll k_0$), Ω is a frequency of coherent photons, k_0 is an averaged propagation constant in square waveguide lattice, δk is associated with overlap couplings between neighboring waveguides and q and p take the values $p = \pi n/N$ and $q = \pi m/N$. Here n and m are integers from 1 to N and thus the total number of modes $M = N^2$. The expectation value of the Hamiltonian $\hat{H}_L$ farther can be presented in the form $H_L = \sum_{j=1}^{M} \varepsilon_j |c_j|^2$. Here $|c_j|^2$ represents the mode occupation, and ε_j is the corresponding eigenvalue. The total power is given via $\mathcal{P} = \sum_{j=1}^{M} |c_j|^2$. The nonlinear interactions between different modes lead to the thermalization of the system to the Rayleigh-Jeans distribution (for the detailed derivation, see Ref.[34]). The temperature T in the model is introduced through the equation

$$|c_j|^2 = -\frac{T}{\varepsilon_j + \mu}, \tag{2}$$

where μ is the chemical potential. The equation of the state of the multimode system reads:

$$U - \mu\mathcal{P} = MT,$$
$$\mathcal{P} = -\sum_{j=1}^{M} \frac{T}{\varepsilon_j + \mu}, \tag{3}$$

where M is the number of the mode. We note that the internal energy of the multitude system and power are conserved quantities defined through the initial distribution of the amplitudes $U = -\sum_{i=1}^{M} \varepsilon_i |c_{i0}|^2$, $\mathcal{P} = \sum_{i=1}^{M} |c_{i0}|^2$. Therefore, two equations Eq.(3) are enough to define two thermodynamic quantities, such as temperature T and chemical potential μ. In dimensionless units the total energy of the system is given by $E = \Omega\mathcal{P}$, where Ω is the frequency of photons. On the other hand $E = \alpha^2 \hbar\Omega M$ where α^2 is the mean photon number per mod estimated as $\alpha^2 = \mathcal{P}/\hbar M$.

If the formation of the thermal state in the multimode optical system is beyond a doubt, then the two-level atom coupled to the multimode optical system should thermalize, too. In what follows, we exploit a two-level atom with experimentally observable level populations as a hyperfine sensor for the detection of thermalization. The two-level atom interacting with the particular j mode is described by the Jaynes–Cummings model [36]:

$$\hat{H}_j = \hbar\Omega\hat{a}^+\hat{a} + \frac{1}{2}\hbar\omega\hat{\sigma}_z + G_j(z)(\hat{\sigma}\hat{a}^+ + \hat{\sigma}^+\hat{a}). \tag{4}$$

Here Ω is the frequency of coherent photons, $G_j(z) =$

$\hbar g|c_j|\cos\left[(k_0+\varepsilon_j)z\right]$ describes the interaction of the two-level atom with the multimode system, z is the distance of the two-level atom from the center of the jth mode. The particular mode j here is chosen randomly. Therefore, we average the obtained solution over the ensemble of all $M = N^2 = 400$ modes and omit index j in the equations for brevity. The states of the two-level atom are given by $|e\rangle = \begin{pmatrix}1\\0\end{pmatrix}$, $|g\rangle = \begin{pmatrix}0\\1\end{pmatrix}$, and $\hat{\sigma}^+ = |e\rangle\langle g|$, $\hat{\sigma} = |g\rangle\langle e|$, and $\hbar = 1$ in what follows. To solve the Schrödinger equation

$$i\frac{\partial|\Psi\rangle}{\partial t} = \hat{H}|\Psi\rangle, \tag{5}$$

we assume that the initial state is the product state of the atom and field and the field is prepared in the coherent state [37, 38] $|\Psi\rangle = |\psi\rangle_a \otimes |\psi\rangle_f = [c_e|e\rangle + c_g|g\rangle] \otimes \sum\limits_{n=0}^{\infty} w_n|n\rangle$, where $w_n = \frac{\alpha^m}{\sqrt{m!}}e^{-\alpha^2/2}$, $|n\rangle$ is the state with n photons, and $|\alpha|^2$ is the mean photon number. From the solution of the Schrödinger equation we construct the density matrix of the system $\rho_j(t) = |\Psi\rangle\langle\Psi|$ and calculate the reduced density matrix of the atom [39]:

$$\hat{\rho}_a^j(t) = \mathrm{Tr}_f(\hat{\rho}^j(t)) = \sum_n \langle n|\hat{\rho}^j(t)|n\rangle, \tag{6}$$

Tr_f means the trace over the states of photonic field. In the explicit form:

$$\begin{aligned}
&\rho_{11}^j(t) = \rho_{00}(0)[1-\alpha(t)] + \rho_{11}(0)\beta(t),\\
&\rho_{00}^j(t) = \rho_{00}(0)\alpha(t) + \rho_{11}(0)[1-\beta(t)],\\
&\rho_{10}^j(t) = \rho_{10}(0)\gamma(t)\\
&\rho_{01}^j(t) = \rho_{01}(0)\gamma^*(t).
\end{aligned} \tag{7}$$

Here we introduced the notations:

$$\begin{aligned}
&C_n(t) = e^{i(\omega-\Omega)t/2}\Big[\cos(\lambda_n t/2) -\\
&i\frac{(\omega-\Omega)}{\lambda_n}\sin(\lambda_n t/2)\Big],\\
&\alpha(t) = \sum_n C_n^*(t)C_n(t),\\
&\beta(t) = \sum_n C_{n+1}^*(t)C_{n+1}(t),\\
&\gamma(t) = \sum_n C_n(t)C_{n+1}(t),
\end{aligned} \tag{8}$$

and the expression of the Rabi frequency has the form $\lambda_n = \sqrt{(\omega-\Omega)^2 + 4(n+1)G_j^2(z)}$, $G_j(z) = \hbar g|c_j|\cos\left[(k_0+\varepsilon_j)z\right]$. We are interested in the diagonal matrix elements, which we define in terms of atomic inversion after averaging over the ensemble of modes:

$$\begin{aligned}
\rho_{11} &= \frac{1}{2}(1+\mathcal{W}),\\
\rho_{22} &= \frac{1}{2}(1-\mathcal{W}).
\end{aligned} \tag{9}$$

Following [40] we present atomic inversion in the form:

$$\begin{aligned}
&\mathcal{W} = \mathcal{A}_0 + \mathcal{A}(t),\\
&\mathcal{A}_0 = \sum_{n=0}^{\infty}\sum_{j=1}^{M}\frac{|\alpha|^{2n}e^{-|\alpha|^2}}{M\cdot n!}\frac{(\omega-\Omega)^2}{\lambda_n^2},\\
&\mathcal{A}(t) = \sum_{n=0}^{\infty}\sum_{j=1}^{M}\frac{|\alpha|^{2n}e^{-|\alpha|^2}}{M\cdot n!}\frac{2(n+1)(\hbar g)^2}{\lambda_n^2}\times\\
&|c_j|^2\left(1+\cos[2(k_0+\epsilon_j)z]\right)\cos(\lambda_n t).
\end{aligned} \tag{10}$$

It is easy to see that only the term $\mathcal{A}(t)$ depends on the time. Therefore, the study of the thermalization process is reduced to the asymptotic limit of $\mathcal{A}_{t\to\infty}$. After performing summation for over the n we deduce:

$$\mathcal{A}_0 = \sum_{j=1}^{M}\frac{(\omega-\Omega)^2}{(\omega-\Omega)^2 + 4|\alpha|^2G_j^2(z)}, \tag{11}$$

while for the time-dependent part, we deduce

$$\begin{aligned}
&\mathcal{A}(t) = \sum_{n=0}^{\infty}\frac{2(\hbar g)^2(n+1)|\alpha|^{2n}e^{-|\alpha|^2}}{M\cdot n!}\mathcal{F}_n(t),\\
&\mathcal{F}_n(t) = \sum_{j=1}^{M}\frac{|c_j|^2}{\lambda_n^2}\left(1+\cos[2(k_0+\varepsilon_j)z]\right)\cos(\lambda_n t).
\end{aligned} \tag{12}$$

The effective atomic temperature is given by

$$T_a = \frac{\hbar\omega}{k_B\ln\left[\frac{1+\mathcal{W}}{1-\mathcal{W}}\right]}. \tag{13}$$

In the high temperature limit all modes are equally populated, meaning that Eq.(2) simplifies as follows: $|\mu| \gg \varepsilon_j$, $|c_j|^2 = T/|\mu| =$const, with $T \gg 1$. Then summation over the ensemble of modes in Eq.(11) and Eq.(12) can be performed analytically and we deduce:

$$\begin{aligned}
&\mathcal{W}(t) = \frac{e^{-\alpha^2}\left(1+\cos(\lambda_0 t)\right)\varepsilon_{max}}{2M} -\\
&\frac{e^{-\alpha^2}\left(1-\cos(\lambda_0 t)\right)\varepsilon_{max}}{2Mz\sqrt{2\xi+1}}\Bigg(\arctan\left[\frac{\tan[z\varepsilon_{max}+k_0]}{\sqrt{2\xi+1}}\right] -\\
&\arctan\left[\frac{\tan[k_0]}{\sqrt{2\xi+1}}\right]\Bigg),
\end{aligned} \tag{14}$$

where we introduced the notation $\xi = \frac{2(\hbar g)^2|c|^2}{(\omega-\Omega)^2}$. From Eq.(14) it is easy to see that $\mathcal{W}(t) \to 0$ as $M \gg 1$ and $\alpha^2 \gg 1$. Then temperature of the atom approaches to the temperature of the modes:

$$T_a = \frac{\hbar\omega}{k_B\mathcal{W}} \to \infty,\ \ T \to \infty. \tag{15}$$

Results and conclusions: For the finite mode temperature case, the atom temperature is distinct from the mode temperature. In Fig.2, we plot the distribution of

TABLE I. The value of A_0 (in bold phase) for different values of power P, internal energy U, chemical potential μ, the value of the mode temperature T and the mean photon number $|\alpha|^2$. The number of the modes $M = N^2 = 400$.

P	U	μ	T	$\lvert\alpha\rvert^2$		
				10	20	50
200	75.689	−7.266	3.822	**0.182**	**0.127**	**0.077**
300	109.750	−7.020	5.539	**0.147**	**0.102**	**0.061**
400	141.250	−6.766	7.117	**0.126**	**0.087**	**0.052**

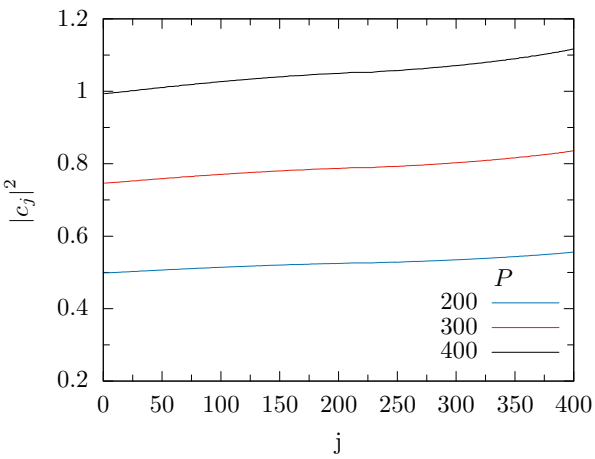

FIG. 2. The stored distribution of the mode amplitudes $|c_j|^2$. Slight increase of the amplitudes with j is a signature of negative chemical potential of the modes.

the mode amplitudes $|c_j|^2$ after thermalization. Amplitudes are sorted in the order of the modes $\varepsilon_{j+1} > \varepsilon_j$. As we see, the values of $|c_j|^2$ are increasing with j meaning the negative chemical potential of the optical multimode system. With increasing of power $\mathcal{P}$, i.e., the energy pumped in the optical modes, the distribution of the amplitudes becomes more uniform because of $T \gg \max(\varepsilon_j)$, $|\mu| \gg \max(\varepsilon_j)$. In Table , we present results for the time-independent part of the inversion $\mathcal{A}_0$, Eq.(10) calculated for the different values of parameters. As we see from the table, with the increasing mode temperature T and mean photon number $|\alpha|^2$, value of $\mathcal{A}_0$ tends to zero, which is a signature of the infinite temperature of the atom (both levels are equally populated). The thermalization process of the atom is described by the time-dependent part of inversion Eq.(12) and is plotted in Figs. 3, 4. As we see from the plots, the dependent part of the inversion decays in time, and instead of the quantum revivals, we see small fluctuations only. Function $\mathcal{F}_n(t)$ in Fig. 3 characterizes decay of partial contributions in Eq.(12) related to the states with a particular number of photons $|n\rangle$, while $\mathcal{A}_n(t)$ in Eq.(4) describes the effect of all states. In the present project, we study the dynamics of the two-level system coupled with the multimode optical system. In particular, we considered a square lattice of optical fibers. We aimed to answer whether we can infer information about the thermalization of optical modes through the thermalization of two-level atoms. After averaging over the set of modes, the dynamic of the two-level system is free of quantum revivals, and that is the signature of thermalization. We showed that the temperature of the two-level system increases with the temperature of optical modes and mean photon number. In the high-temperature limit of optical modes, the temperature of the level system tends to be infinity, and level populations are equal.

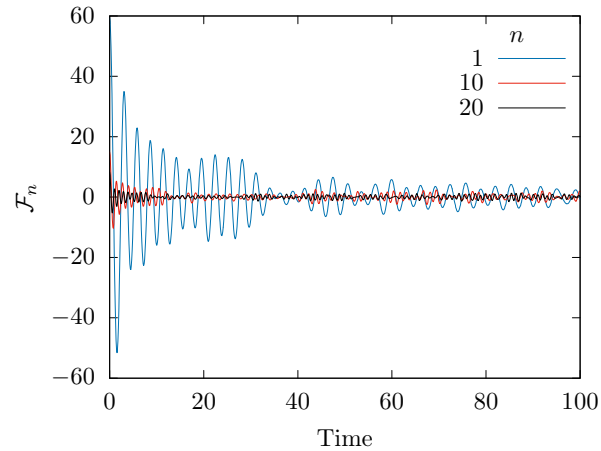

FIG. 3. Decay of partial contributions$\mathcal{F}_n(t)$ in Eq.(12) related to the states with a particular number of photons $|n\rangle$, for different n and mean photon number $|\alpha|^2 = 10$. Initial power is equal to $\mathcal{P} = 200$.

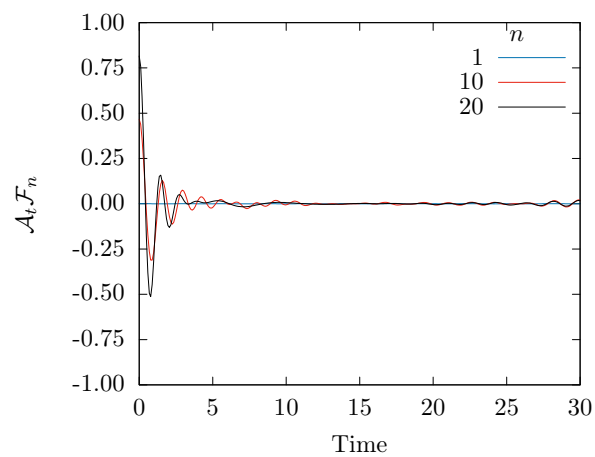

FIG. 4. The time-dependent part of the level inversion Eq.(12) $\mathcal{A}(t)$ summed up for the states from the single 1 up to $n = 20$ photons. The mean photon number is equal to $|\alpha|^2 = 10$, $P = 200$.

[1] M. Srednicki, Chaos and quantum thermalization, Phys. Rev. E **50**, 888 (1994).

[2] S. Yuan, M. I. Katsnelson, and H. De Raedt, Origin of the canonical ensemble: Thermalization with decoherence, J. Phys. Soc. Jpn. **78**, 094003 (2009).

[3] F. Jin, H. De Raedt, S. Yuan, M. I. Katsnelson, S. Miyashita, , and M. K., Approach to equilibrium in nano-scale systems at finite temperature, J. Phys. Soc. Jpn. **79**, 124005 (2010).

[4] A. V. Ponomarev, S. Denisov, and P. Hänggi, Thermal equilibration between two quantum systems, Phys. Rev. Lett. **106**, 010405 (2011).

[5] G. G. Pyrialakos, H. Ren, P. S. Jung, M. Khajavikhan, and D. N. Christodoulides, Thermalization dynamics of nonlinear non-hermitian optical lattices, Phys. Rev. Lett. **128**, 213901 (2022).

[6] C. Shi, T. Kottos, and B. Shapiro, Controlling optical beam thermalization via band-gap engineering, Phys. Rev. Res. **3**, 033219 (2021).

[7] A. Marques Muniz, F. Wu, P. Jung, M. Khajavikhan, D. Christodoulides, and U. Peschel, Observation of photon-photon thermodynamic processes under negative optical temperature conditions, Science **379**, 1019 (2023).

[8] J. M. Deutsch, Quantum statistical mechanics in a closed system, Phys. Rev. A **43**, 2046 (1991).

[9] J. M. Deutsch, Eigenstate thermalization hypothesis, Reports on Progress in Physics **81**, 082001 (2018).

[10] R. Steinigeweg, A. Khodja, H. Niemeyer, C. Gogolin, and J. Gemmer, Pushing the limits of the eigenstate thermalization hypothesis towards mesoscopic quantum systems, Phys. Rev. Lett. **112**, 130403 (2014).

[11] M. Rigol, V. Dunjko, and M. Olshanii, Thermalization and its mechanism for generic isolated quantum systems, Nature **452**, 854 (2008).

[12] L. D'Alessio, Y. Kafri, A. Polkovnikov, and M. Rigol, From quantum chaos and eigenstate thermalization to statistical mechanics and thermodynamics, Advances in Physics **65**, 239 (2016).

[13] J.-S. Caux and F. H. L. Essler, Time evolution of local observables after quenching to an integrable model, Phys. Rev. Lett. **110**, 257203 (2013).

[14] P. Łydżba, M. Mierzejewski, M. Rigol, and L. Vidmar, Generalized thermalization in quantum-chaotic quadratic hamiltonians, Phys. Rev. Lett. **131**, 060401 (2023).

[15] R. B. S, V. Mukherjee, U. Divakaran, and A. del Campo, Universal finite-time thermodynamics of many-body quantum machines from kibble-zurek scaling, Phys. Rev. Research **2**, 043247 (2020).

[16] N. Jaseem, M. Hajdušek, V. Vedral, R. Fazio, L.-C. Kwek, and S. Vinjanampathy, Quantum synchronization in nanoscale heat engines, Phys. Rev. E **101**, 020201 (2020).

[17] K. Brandner and K. Saito, Thermodynamic geometry of microscopic heat engines, Phys. Rev. Lett. **124**, 040602 (2020).

[18] M. Scandi, H. J. D. Miller, J. Anders, and M. Perarnau-Llobet, Quantum work statistics close to equilibrium, Phys. Rev. Research **2**, 023377 (2020).

[19] G. Benenti, G. Casati, and J. Wang, Power, efficiency, and fluctuations in steady-state heat engines, Phys. Rev. E **102**, 040103 (2020).

[20] O. Abah, M. Paternostro, and E. Lutz, Shortcut-to-adiabaticity quantum otto refrigerator, Phys. Rev. Research **2**, 023120 (2020).

[21] R. Kosloff and Y. Rezek, The quantum harmonic otto cycle, Entropy **19**, 136 (2017).

[22] T. Denzler and E. Lutz, Efficiency fluctuations of a quantum heat engine, Phys. Rev. Research **2**, 032062 (2020).

[23] A. del Campo and K. Kim, Focus on shortcuts to adiabaticity, New Journal of Physics **21**, 050201 (2019).

[24] K. Ono, S. N. Shevchenko, T. Mori, S. Moriyama, and F. Nori, Analog of a quantum heat engine using a single-spin qubit, Phys. Rev. Lett. **125**, 166802 (2020).

[25] M. Naghiloo, D. Tan, P. M. Harrington, J. J. Alonso, E. Lutz, A. Romito, and K. W. Murch, Heat and work along individual trajectories of a quantum bit, Phys. Rev. Lett. **124**, 110604 (2020).

[26] D. Guéry-Odelin, A. Ruschhaupt, A. Kiely, E. Torrontegui, S. Martínez-Garaot, and J. G. Muga, Shortcuts to adiabaticity: Concepts, methods, and applications, Rev. Mod. Phys. **91**, 045001 (2019).

[27] O. Abah and E. Lutz, Energy efficient quantum machines, EPL (Europhysics Letters) **118**, 40005 (2017).

[28] O. Abah and E. Lutz, Performance of shortcut-to-adiabaticity quantum engines, Phys. Rev. E **98**, 032121 (2018).

[29] M. Azimi, L. Chotorlishvili, S. K. Mishra, T. Vekua, W. Hübner, and J. Berakdar, Quantum otto heat engine based on a multiferroic chain working substance, New Journal of Physics **16**, 063018 (2014).

[30] L. Chotorlishvili, M. Azimi, S. Stagraczyński, Z. Toklikishvili, M. Schüler, and J. Berakdar, Superadiabatic quantum heat engine with a multiferroic working medium, Physical Review E **94**, 032116 (2016).

[31] L. Chotorlishvili, Z. Toklikishvili, and J. Berakdar, Thermal entanglement and efficiency of the quantum otto cycle for the su (1, 1) tavis–cummings system, Journal of Physics A: Mathematical and Theoretical **44**, 165303 (2011).

[32] S. Stagraczyński, L. Chotorlishvili, M. Schüler, M. Mierzejewski, and J. Berakdar, Many-body localization phase in a spin-driven chiral multiferroic chain, Phys. Rev. B **96**, 054440 (2017).

[33] R. Khomeriki, L. Chotorlishvili, B. A. Malomed, and J. Berakdar, Creation and amplification of electromagnon solitons by electric field in nanostructured multiferroics, Phys. Rev. B **91**, 041408 (2015).

[34] F. O. Wu, A. U. Hassan, and D. N. Christodoulides, Thermodynamic theory of highly multimoded nonlinear optical systems, Nature Photonics **13**, 776 (2019).

[35] L. G. Wright, F. O. Wu, D. N. Christodoulides, and F. W. Wise, Physics of highly multimode nonlinear optical systems, Nature Physics **18**, 1018 (2022).

[36] E. T. Jaynes and F. W. Cummings, Comparison of quantum and semiclassical radiation theories with application to the beam maser, Proceedings of the IEEE **51**, 89 (1963).

[37] A. M. Perelomov, *Generalized Coherent States and Their Applications*, Vol. 1 (Springer, 1986).

[38] W.-M. Zhang, D. H. Feng, and R. Gilmore, Coherent states: Theory and some applications, Rev. Mod. Phys.

62, 867 (1990).

[39] A. Smirne and B. Vacchini, Nakajima-zwanzig versus time-convolutionless master equation for the non-markovian dynamics of a two-level system, Phys. Rev. A **82**, 022110 (2010).

[40] A. A. Karatsuba and E. A. Karatsuba, A resummation formula for collapse and revival in the jaynes–cummings model, Journal of Physics A: Mathematical and Theoretical **42**, 195304 (2009).